Supplemental Material

Crystal structure and mutational analysis of *Mycobacterium smegmatis* FenA highlight active site amino acids and three metal ions essential for flap endonuclease and 5' exonuclease activities

Maria Loressa Uson, Ayala Carl, Yehuda Goldgur, and Stewart Shuman

Supplemental Tables S1 and S2

Supplemental Figures S1, S2, S3, and S4

Table S1

Crystallographic data and refinement statistics

	SeMet-WT	D125N	D148N	D208N
Data collection				
Beamline	APS 24-ID-C	APS 24-ID-E	APS 24-ID-E	APS 24-ID-C
Space group	$P2_1$	$P2_1$	$P2_1$	$P2_1$
Cell dimensions a, b, c (Å) α, β, γ (°)	 63.1, 39.8, 68.2 90, 108.9, 90	 63.2, 39.9, 68.4 90, 108.8, 90	 63.4, 40.1, 68.4 90, 109.1, 90	 63.2, 39.9, 68.4 90, 109.1, 90
Resolution (Å)	50–1.8(1.85-1.8)	50–2.2 (2.25–2.2)	50–1.8 (1.85-1.8)	50–1.9 (1.95-1.9)
Wavelength (Å)	0.9791	0.9792	0.9792	0.9791
R_{pim}	0.060 (0.447)	0.075 (0.420)	0.031 (0.133)	0.068 (0.378)
CC(1/2)	0.997 (0.600)	0.995 (0.810)	0.995 (0.915)	0.996 (0.620)
$\langle I \rangle / \langle \sigma I \rangle$	20.9 (2.0)	5.9 (1.4)	22.2 (3.0)	10.0 (1.5)
Completeness (%)	98.8 (97.4)	99.0 (99.9)	98.0 (87.2)	98.9 (97.1)
Redundancy	5.4 (3.1)	4.1 (4.1)	3.9 (2.8)	4.2 (3.3)
Unique reflections	29804	16681	29647	25196
Phasing				
HA sites	2 Se, 1 Mn			
Figure of merit	0.338			
Refinement				
R_{work} / R_{free}	0.174 / 0.205	0.177 / 0.226	0.157 / 0.193	0.185 / 0.220
B-factors (Å^2) Average/Wilson	28.5 / 23.8	37.7 / 31.3	23.9 / 19.1	24.1 / 20.3
RMS deviations bond lengths (Å) bond angles (°)	 0.006 0.887	 0.007 0.938	 0.006 0.903	 0.007 0.977
Ramachandran plot % favored % allowed % outliers	 99.4 0.6 0	 98.1 1.6 0.3	 97.8 2.2 0	 98.7 1.3 0
Model contents				
Protomers / ASU	1	1	1	1
Protein residues	316	316	316	316
Ions	4 Mn	3 Mn	3 Mn	3 Mn, 1 phosphate
Water	271	251	431	292
PDB ID	6C33	6C34	6C35	6C36

Values in parentheses refer to the highest resolution shell.

R_{free} set consists of 10% of data chosen randomly against which structures was not refined.

Table S2

Closest Structural Homologs of FenA

Protein	pdb ID	Z score	root mean square deviation	% identity
Escherichia coli ExoIX	3ZDD	25.1	2.0 Å at 243 Cα positions	25
Taq Polymerase	1TAU	23.1	3.1 Å at 254 Cα positions	26
T5 Fen	1EXN	22.5	2.7 Å at 242 Cα positions	21
Methanopyrus kandleri FEN1	4WA8	18.7	3.3 Å at 251 Cα positions	20
Archaeoglobus fulgidus FEN1	1RXV	18.3	3.9 Å at 254 Cα positions	17
T4 Fen (RNaseH)	2IHN	18.2	3.1 Å at 247 Cα positions	16
Methanococcus jannaschii FEN1	1A77	17.6	3.9 Å at 253 Cα positions	18
Human FEN1	3Q8M	17.5	4.3 Å at 264 Cα positions	16
Pyrococcus furiosus FEN1	1B43	17.2	3.5 Å at 249 Cα positions	16
Sulfolobus solfataricus FEN1	2IZO	15.9	3.2 Å at 217 Cα positions	18
Saccharomyces cerevisiae Rad2	4Q0Z	15.9	4.2 Å at 250 Cα positions	18
Human GEN1	5T9J	15.5	3.4 Å at 253 Cα positions	15
Human ExoI	5V0D	13.6	3.7 Å at 227 Cα positions	13
Caenorhabditis elegans XRN2	5FIR	10.7	4.3 Å at 247 Cα positions	11

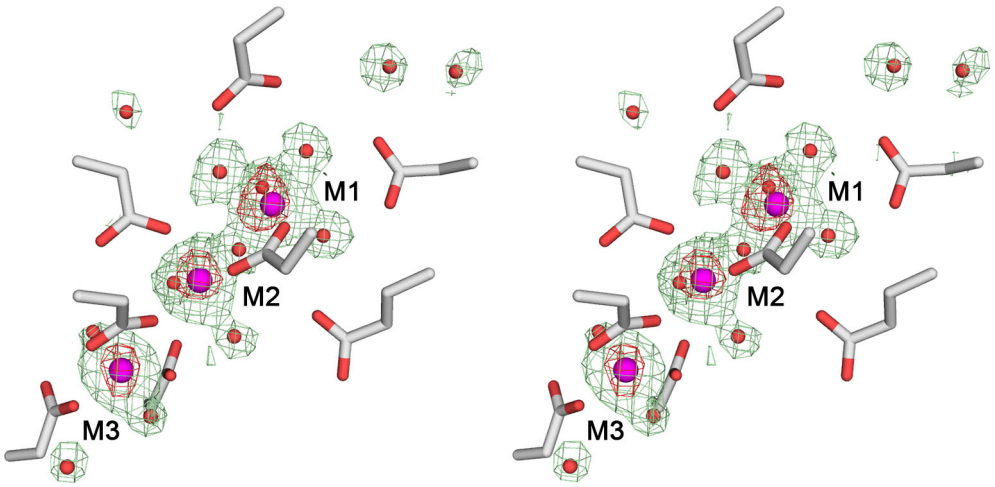

Figure S1. Stereo view of a simulated annealing Fo-Fc omit map (green mesh contoured at 3σ) and an anomalous difference map (red mesh contoured at 4σ) affirm the presence of three manganese ions (M1, M2, and M3, magenta spheres) in the wild-type FenA active site. Waters are depicted as red spheres. The eight conserved acidic side chains that engage the metal ions are shown as stick models.

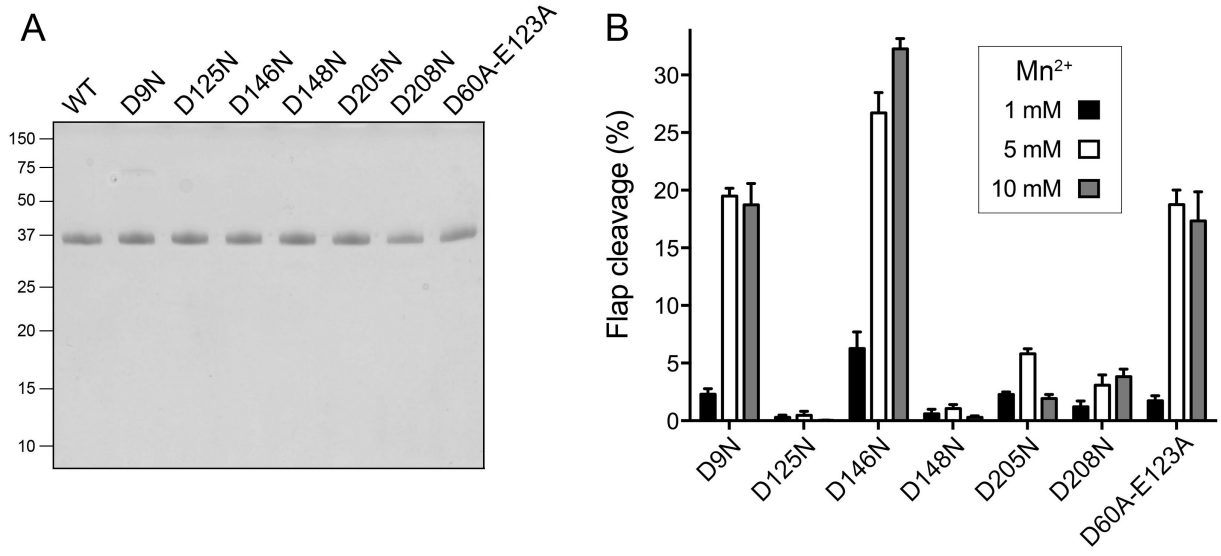

Figure S2. FenA Asp-to-Asn mutants and tests of rescue by increasing manganese concentration. (A) Aliquots (5 µg) of the preparations of wild-type (WT) FenA and the indicated Asp-to-Asn mutants as well as the D60A-E123A double-alanine mutant were analyzed by SDS-PAGE. The Coomassie blue-stained gel is shown. The positions and sizes (in kilodaltons) of marker polypeptides are indicated on the left. (B) Reaction mixtures (10 µl) containing 20 mM Tris-HCl, pH 8.0, 50 mM NaCl, 1, 5 or 10 mM $MnCl_2$ as specified, 1 mM DTT, 1 pmol (100 nM) ^{32}P-labeled flap-nick substrate, and 10 pmol (1 µM) FenA mutant were incubated for 30 min at 37°C. The extents of flap cleavage by each mutant are plotted in bar graph format as a function of increasing manganese concentration. Each datum is the average of three separate experiments ±SEM.

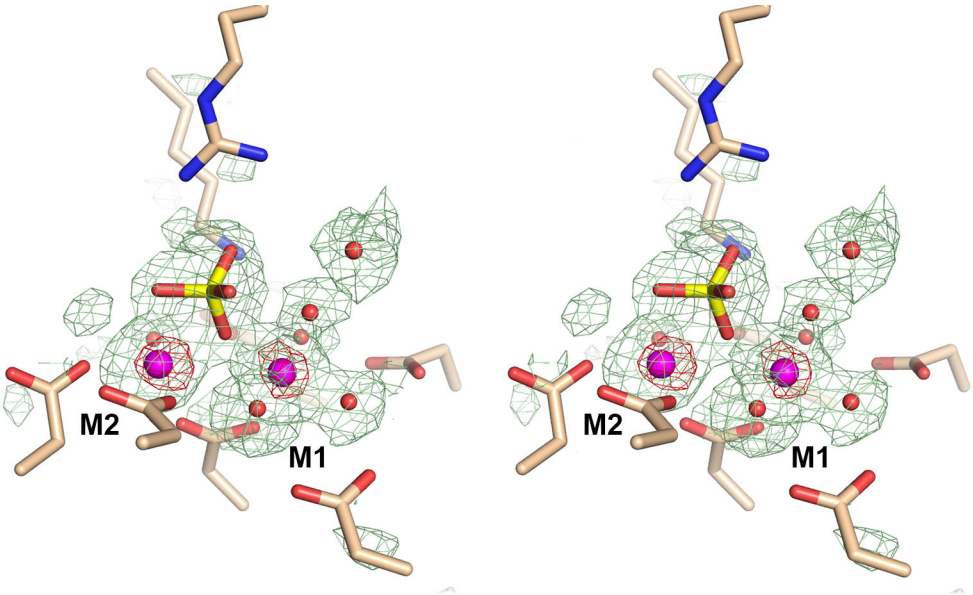

Figure S3. Stereo view of a simulated annealing Fo-Fc omit map (green mesh contoured at 2.5σ) and an anomalous difference map (red mesh contoured at 4σ) of the D208N active site in the region surrounding the M1 and M2 manganese ions (magenta spheres). A tetrahedron-shaped density between M1 and M2 is modeled as a phosphate anion. Waters are depicted as red spheres. Amino acid side chains are shown as stick models with beige carbons.

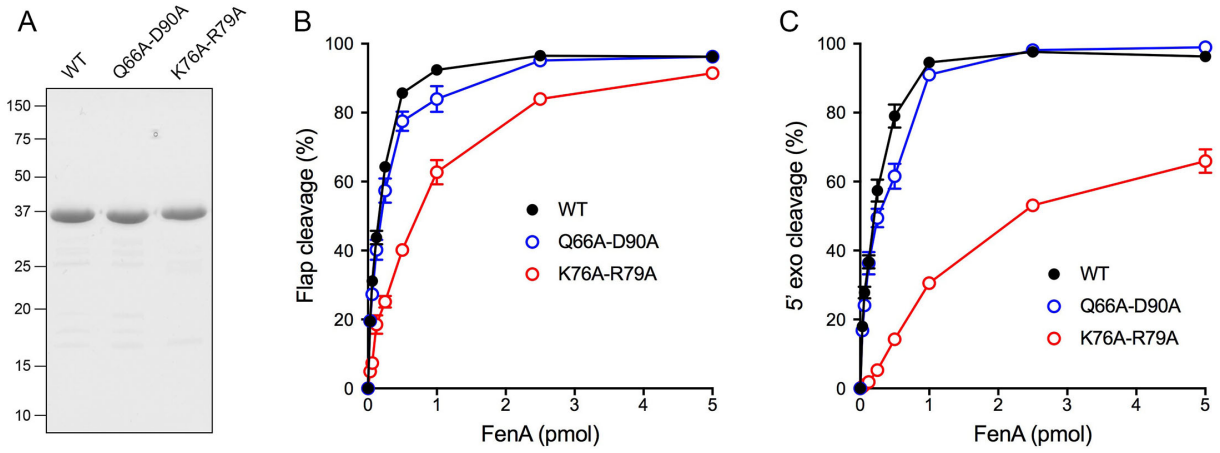

Figure S4. Effect of mutations of phosphate-binding and M4-binding amino acids on FenA activity. (A) Aliquots (5 µg) of the preparations of wild-type (WT) FenA and the indicated double-alanine mutants were analyzed by SDS-PAGE. The Coomassie blue-stained gel is shown. The positions and sizes (in kilodaltons) of marker polypeptides are indicated on the left. (B and C) Mutational effects on flap endonuclease (B) and 5' exonuclease activity (C). Reaction mixtures (10 µl) containing 20 mM Tris-HCl, pH 8.0, 50 mM NaCl, 1 mM $MnCl_2$, 1 mM DTT, and 1 pmol (100 nM) of either ^{32}P-labeled 10-mer flap-nicked duplex DNA (panel B) or ^{32}P-labeled nicked duplex DNA (panel C), and increasing amounts of wild-type (WT) or mutant FenA were incubated for 30 min at 37°C. The reaction products were analyzed by urea-PAGE and visualized and quantified by scanning the gel with a phosphorimager. The extents of cleavage of the substrates are plotted as a function of input FenA. Each datum is the average of three independent titration experiments ± SEM.